

Incommensurate structure in the Bi-Sr-Ca-Cu-O 80-K superconductor

T. M. Shaw, S. A. Shivashankar, S. J. La Placa, J. J. Cuomo, T. R. McGuire, R. A. Roy, K. H. Kelleher, and D. S. Yee

IBM Research Division, Thomas J. Watson Research Center, Yorktown Heights, New York 10598

(Received 12 February 1988)

We report on the structure and characterization of the major phase in the Bi-Sr-Ca-Cu-O system that becomes superconducting below 80 K. A superlattice modulation in the structure that is incommensurate with a tetragonal perovskite-based subcell is observed using electron diffraction. High-resolution imaging indicates that the modulation occurs primarily in bismuth-rich layers in the structure.

The observation of high-temperature superconductivity in the $\text{La}_{1-x}\text{Ba}_x(\text{Sr}_x)\text{CuO}_4$ (Ref. 1) and $\text{YBa}_2\text{Cu}_3\text{O}_{7-\delta}$ (Ref. 2) compounds has led to a search for superconductivity in other oxide systems. Michel *et al.*³ recently reported superconductivity in the non-rare-earth-containing $\text{Bi}_2\text{Sr}_2\text{Cu}_2\text{O}_{7+\delta}$ oxide with transition temperatures as high as 22 K. A new Bi-Sr-Ca-Cu-O composition has been found by Maeda, Tanaka, Fukutomi, and Asano⁴ to exhibit a complete superconductivity transition at 80 K with well-defined resistance drops starting as high as 115 K. The observation of superconductivity in this system has been confirmed by Chu *et al.*⁵ The phase has been identified by Hazen *et al.*⁶ who report unit-cell dimensions of $5.44 \times 27.2 \times 30.78$ Å for the structure which corresponds to a superlattice of a $5.41 \times 5.439 \times 30.78$ -Å *A*-centered orthorhombic subcell.

We report on the structure and characterization of the superconducting phase in the Bi-Sr-Ca-Cu-O system. Although in general, our observations support those of Hazen *et al.*⁶ high-resolution electron microscopy and electron-diffraction observations indicate a superlattice modulation is present that is incommensurate with the perovskite-related subcell.

Compositions with a variety of different empirical formulas based on the Maeda *et al.* and Michel *et al.* formulations were prepared in order to explore formation of superconducting phases in the Bi-Sr-Ca-Cu-O system. In the present paper we report primarily on an investigation of the superconducting phase observed in a material prepared with molar ratios of Bi:Sr:Ca:Cu = 1:1:2:2. The material was prepared from a mixture of Bi_2O_3 (99.99%), SrCO_3 (99.99%), CaCO_3 (99.9%), and CuO (99.9%), by calcining in air at 800°C followed by a sintering in air at 860°C. The pellets quenched from this temperature were found to be dense, due to proximity to the melting point. Metallographic examination indicated the presence of three phases, one of them consisting of acicular grains and connected across the specimen. The presence of Ca_2CuO_3 in the sample was determined from x-ray powder-diffraction data. Electron microprobe analysis confirmed the presence of the cuprate, as well as indicating that the acicular grains contained all four cations in the molar proportion Bi:Sr:Ca:Cu=8:6.7:3:7.2. This phase was assumed to be responsible for the observed superconductivity. The oxygen content of the phase is not yet known.

Subsequent studies have shown that single-phase superconducting material can be made near this composition. Further details of the characterization of the superconducting properties of the phase will be reported in a separate paper. The nominal cation composition of the third phase was found to be Ca:Sr:Cu = 1:1:3, with a trace of bismuth. This composition was synthesized and found to be semiconducting and was not investigated further.

A four-probe resistance measurement made on the material showed a gradual superconducting transition, with zero resistance reached at 69 K. Susceptibility measurement in a SHE superconducting quantum interference device (SQUID) magnetometer showed a small diamagnetic signal beginning at 105 K, with a 29% diamagnetic shielding at 4.2 K. The majority of the change in magnetization was observed to occur at about 80 K.

Transmission electron microscopy and electron diffraction were used to examine single-crystal grains in powdered and ion-milled samples. The powdered samples were prepared by depositing crushed material on carbon support films. An ion-milled sample of the 1:1:2:2 composition was prepared from a slice of bulk material that had been mechanically thinned to 100 μm. The slice was dimpled close to perforation, mounted on a gold support grid, and then ion milled to perforation using 6-kV argon ions. To minimize ion-milling damage, 3-kV argon ions were used for the final thinning. The specimens were examined using a Philips 430T electron microscope operating at 300 kV.

Grains having the known Ca_2CuO_3 and CaCu_2O_3 structures were identified by electron diffraction in the 1:1:2:2 material. In addition, a large unit-cell structure was observed. Strong texturing during the deposition of crushed material on the carbon support grids prevented the observation of all orientations of the crystals in the crushed samples; however, in an ion-milled sample all orientations of the crystals could be reached. The unknown phase was readily identified by its characteristic morphology consisting of clusters of thin plates separated by low-angle grain boundaries. X-ray energy-dispersive spectroscopy analysis indicated that the phase contained significant amounts of all four cations.

Electron-diffraction patterns from three mutually perpendicular zone axes of the crystals are shown in Figs.

1(a)–1(c). The primary reflections in the electron-diffraction patterns can be indexed using a body-centered unit cell of $a = 3.8 \text{ \AA}$, $b = 3.8 \text{ \AA}$, $c = 31.0 \text{ \AA}$ corresponding to a subcell that is approximately $1 \times 1 \times 8$ of the unit cell of a perovskite. The presence of weaker superlattice-type reflections indicate a larger unit cell, rotated 45° from the subcell, with $a = 5.4 \text{ \AA}$, $b = 25.8 \text{ \AA}$, $c = 31.0 \text{ \AA}$, similar to that identified by Michel *et al.*³ for the $\text{Bi}_2\text{Sr}_2\text{Cu}_2\text{O}_{7+\delta}$ structure only with a shorter c axis. In the [001] zone axis pattern in Fig. 1(a), the (100) superlattice reflection is present with weak intensity. The [010] pattern in Fig. 1(b) clearly shows, however, that the reflection is absent and that its presence in the [001] zone axis pattern is caused by streaking along the c^* axis of the reciprocal lattice. Similarly, streaking along the c^* axis can explain the weak intensity observed at the (010) positions in the [001] zone axis pattern. In some patterns, diffuse maxima in the intensity along the streaks can be seen at the (010) and (001) positions shown in the enlarged view of the [100] zone axis pattern in Fig. 1(d). The observations indicate that only reflections for which $h+k+l=2n$ are present and that the superlattice unit cell is body centered. The diffuse intensity maxima in the streaks indicate that further ordering of the structure may also be occurring.

Using the cell obtained from electron diffraction, ten lines in the x-ray powder pattern could be assigned uniquely to the tetragonal structure. Refined lattice constants, obtained from a least-squares fit to the powder-diffraction peaks, are $a = 3.822(2) \text{ \AA}$ and $c = 30.72(2) \text{ \AA}$.

An interesting feature of the electron-diffraction patterns is the fall-off in intensity of the superlattice re-

fections along the b^* axis seen in the enlarged [100] pattern in Fig. 1(d). The intensity indicates that the crystal contains a smoothly varying modulation with a wavelength much larger than the perovskite-based substructure. From accurate measurement of the spacing of the rows of superlattice reflections along the b^* axis we find that the wavelength of the modulation is incommensurate with the 2.7-\AA spacing of (110) perovskite subcell reflections. From the measurements, we estimate the modulation to have a wavelength of 25.8 \AA or 9.56 times the spacing of the (110) perovskite planes at room temperature. Cooling of the ion-milled specimen to 110 K in a liquid-nitrogen stage produced no measurable change in the spacing of the superlattice reflections. In order to determine the generality of the incommensurability of the superlattice, diffraction patterns from the superconducting phase present in three other compositions were examined. In each case, a splitting of ($0h0$)-type reflections characteristic of the incommensurate modulation was observed in [001] diffraction patterns.

Lattice imaging was used to examine two different orientations of the structure. Rapid damage of the structure in the electron beam and the presence of a thick amorphous damaged layer on the ion-beam-thinned samples prevented really high-quality images from being obtained from this structure. To minimize the damage, images were recorded after only short exposures of the areas to the electron beam (typically less than a minute). The focus conditions used for both the images shown was such that the first contrast transfer interval of the microscope extended beyond the 2.7-\AA spacing of the (110) perovskite planes. The form of the transfer function was subsequently confirmed by Fourier analysis of the amorphous background contrast that appeared in the images.

An image of the structure along the [100] direction in the perovskite-based subcell reveals pairs of closely spaced rows of dark dots with a spacing between the pairs of $\approx 15.5 \text{ \AA}$ (Fig. 2). The half-spacing offset between rows of dots and the relative positioning of the pairs of rows are

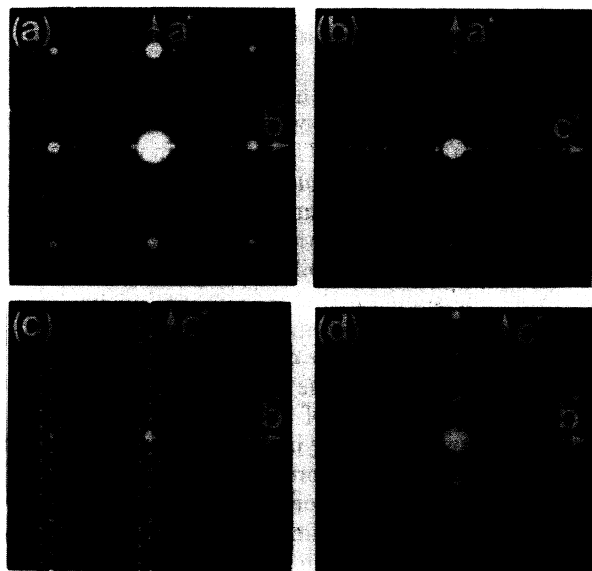


FIG. 1. Electron diffraction patterns taken from three mutually perpendicular orientations of crystals of the unknown phase in the 1:1:2:2 composition. The orientations indexed with respect to the superlattice cell are (a) [001], (b) [010], and (c) [100]. In the enlargement of the portion of the [100] pattern shown in (d) streaking along the c^* axis is evident as well the incommensurate spacing of the superlattice reflections along the b^* axis.

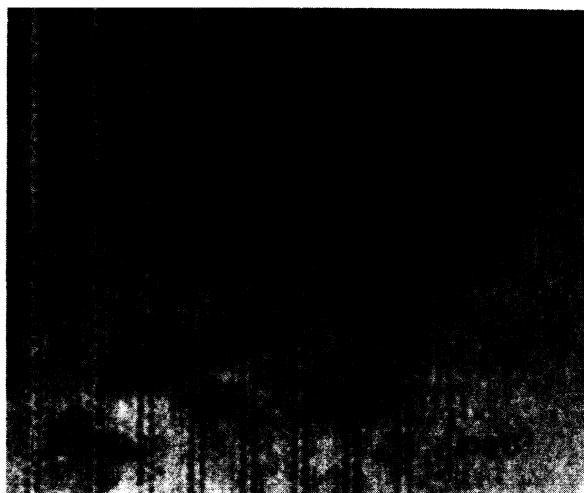


FIG. 2. High-resolution image along a [100] direction of the perovskite-based subcell. In the thinnest areas parallel lines of dark spots indicate layering of the bismuth in the structure.

consistent with the structure suggested by Michel *et al.*,³ in which the heavy bismuth ions occur primarily in $(\text{Bi}_2\text{O}_2)^{2+}$ layers joining the perovskite blocks. The shorter 31.1 Å spacing in the present structure suggest that only two or three layers of octahedra separate the bismuth-containing layers.

In images from a second orientation, [100] of the superlattice cell, pairs of dark lines that are consistent with the proposed layering of the bismuth are again observed in the thinnest regions of the specimen (Fig. 3). Modulations in the intensity in the lines with a ≈ 25.8 -Å period are observed suggesting that the incommensurate period in the structure comes primarily from a modulation in the bismuth-rich layers. The offset in modulations between adjacent layers is approximately half a modulation spacing but varies locally across the crystal. In many regions, the offset in the modulations is consistently less than half the modulation spacing resulting in local regions that have monoclinic symmetry. This structure gives rise to the possibility of twinlike structures in the crystals in which the sense of the offset switches across an (001) plane of the structure. Some evidence for the formation of such twins is seen in the splitting of the (020)-type reflections in the [100] zone axis-diffraction patterns.

It is unclear from the present images whether two or three perovskite blocks are present between the bismuth-containing layers. The spacing of the layers is consistent with there being three perovskite layers if they are undistorted. The possibility that there are only two layers cannot be ruled out if the octahedra are significantly distorted. Indeed, the microprobe analysis of the superconducting phase is more consistent with a copper-poor structure containing only two copper layers for every $(\text{Bi}_2\text{O}_2)^{2+}$ layer. In several regions of the crystals, isolated layers with larger block spacings were observed. The streaking along the c^* direction in the diffraction patterns is probably caused by a combination of such stacking faults and the imperfect correlation between the modulations in adjacent blocks of the structure. It is significant that in each of more than 15 regions lattice imaged in (100), (010) orientations of the supercell and the (100) orientation of the perovskite-based subcell, the perovskite blocks and the bismuth-containing layers appear continuous in two dimensions and are uninterrupted by defects in the crystals.

Two possibilities exist for the structuring of the interperovskite layers. In the first, the bismuth ions lie in square pyramid sites, the apexes of which share oxygens with octahedra in the adjacent perovskite layers as suggested by Michel *et al.* for the $\text{Bi}_2\text{Sr}_2\text{Cu}_2\text{O}_{7+\delta}$ oxide. A second possibility is that bismuth ions lie at positions slightly displaced from the cage sites of the adjacent perovskite blocks as in bismuth titanate structures first described by Aurivillius.⁷ Both structures are consistent with the lattice images and, therefore, we are unable to distinguish between the two structures at the present time. Analogy with the Aurivillius phases suggests that the present structure could be one of a series of intergrowth structures in which the number of perovskite blocks between the $(\text{Bi}_2\text{O}_2)^{2+}$ is varied. Indeed the 48-Å dimension of the unit cell of the $\text{Bi}_2\text{Sr}_2\text{Cu}_2\text{O}_{7+\delta}$ oxide suggests

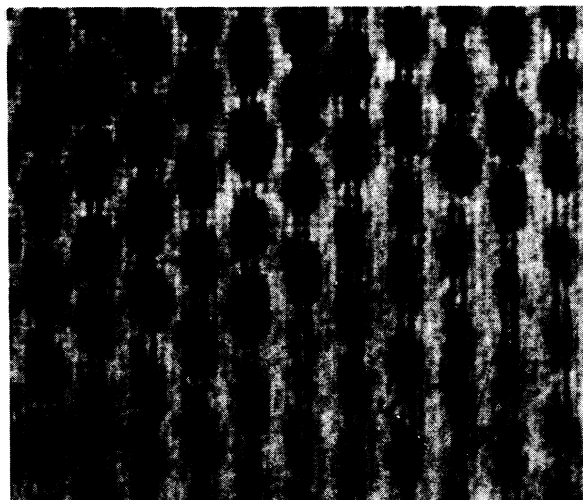


FIG. 3. High-resolution image along the [100] direction of the superlattice cell. The bismuth-containing layers are evident pairs of dark lines. Modulation of contrast along the lines suggests that there is a 25.8-Å modulation in the concentration of bismuth in these layers that is incommensurate with the perovskite substructure.

that it is the five-perovskite-layer structure in such a series.

The modulation in contrast of the dark lines seen in the (100) (superlattice) orientation lattice image in Fig. 3 indicates that the bismuth in the $(\text{Bi}_2\text{O}_2)^{2+}$ layers is not uniformly distributed in the layer. It is possible that the observed contrast comes from displacements of the bismuth cations from their ideal sites, as might arise, for example, from coupling to an incommensurate charge-density wave. It is unlikely, however, that this mechanism could produce a sufficiently pronounced variation contrast to account for the images. The contrast modulation could also be produced by vacant bismuth sites or substitution of strontium or calcium for bismuth in the bismuth-rich layers. Detailed image simulations are needed to determine which, if any, of these possibilities is correct.

A distinct possibility is that the composition modulation only develops on cooling from high temperatures and that at higher temperatures the composition of the layers is more uniform. If this is the case, it may be possible to control the precise form of the superlattice using heat treatments as well as by varying the composition. There is no direct evidence linking presence of the superlattice to the suppression or enhancement of the superconducting properties at the present time. However, the possibility that the superlattice plays an important role in controlling the superconducting behavior cannot be ruled out.

We are grateful to R. Beyers, J. B. Torrance, and A. P. Malozemoff for stimulating discussions and to W. Krakow for assistance with the image analysis. We would also like to thank C. Kroll for her technical assistance.

- ¹J. G. Bednorz and K. A. Müller, *Z. Phys. B* **64**, 189 (1986).
- ²M. K. Wu, J. R. Ashburn, C. J. Torng, P. H. Hor, R. L. Meng, L. Gao, Z. J. Huang, Y. Q. Wang, and C. W. Chu, *Phys. Rev. Lett.* **58**, 908 (1987).
- ³C. Michel, M. Hervieu, M. M. Borel, A. Grandin, F. Deslandes, J. Provost, and B. Raveau, *Z. Phys. B* **68**, 412 (1987).
- ⁴A. H. Maeda, Y. Tanaka, N. Fukutomi, and T. Asano, *Jpn. J. Appl. Phys.* **27**, L209 (1988).
- ⁵C. W. Chu, J. Bechtold, L. Gao, P. H. Hor, Z. J. Huang, R. L. Meng, Y. Y. Sun, Y. Q. Wang, and Y. Y. Xue, *Phys. Rev. Lett.* **60**, 941 (1988).
- ⁶R. M. Hazen, C. T. Prewitt, R. J. Angel, N. L. Ross, L. W. Finger, C. G. Hadjiaicos, D. R. Veblen, P. J. Heanery, H. Hor, R. L. Meng, Y. Y. Sun, Y. Q. Wang, Y. Y. Xue, Z. J. Huang, L. Gao, J. Bechtold, and C. W. Chu, *Phys. Rev. Lett.* **60**, 1174 (1988)
- ⁷B. Aurivillius, *Arkiv Kemi* **1**, 463 (1949); **1**, 499 (1949); **2**, 519 (1950); **5**, 39 (1952).

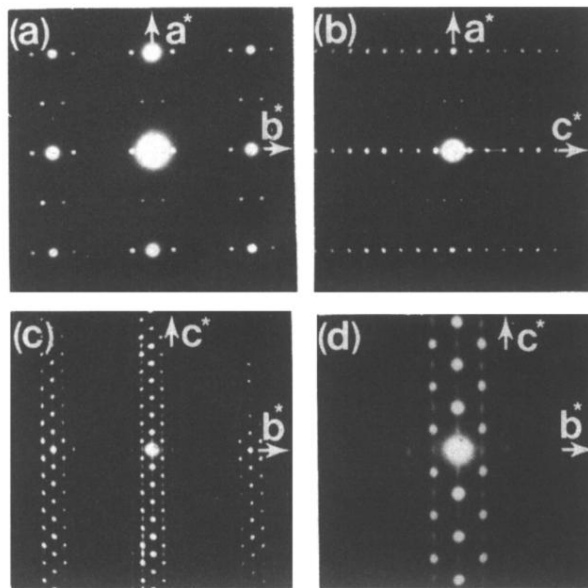


FIG. 1. Electron diffraction patterns taken from three mutually perpendicular orientations of crystals of the unknown phase in the 1:1:2:2 composition. The orientations indexed with respect to the superlattice cell are (a) [001], (b) [010], and (c) [100]. In the enlargement of the portion of the [100] pattern shown in (d) streaking along the c^* axis is evident as well the incommensurate spacing of the superlattice reflections along the b^* axis.

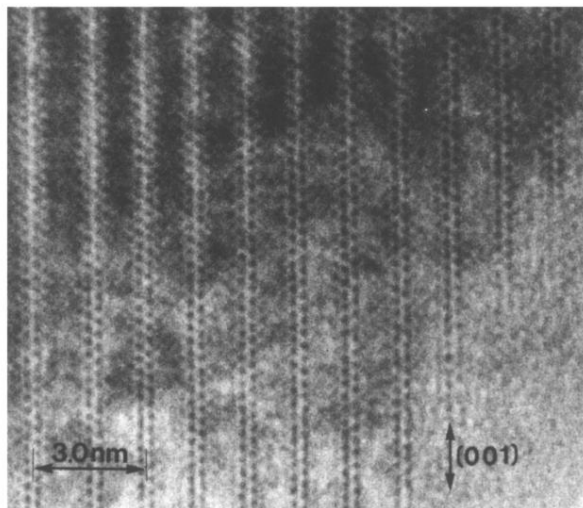


FIG. 2. High-resolution image along a [100] direction of the perovskite-based subcell. In the thinnest areas parallel lines of dark spots indicate layering of the bismuth in the structure.

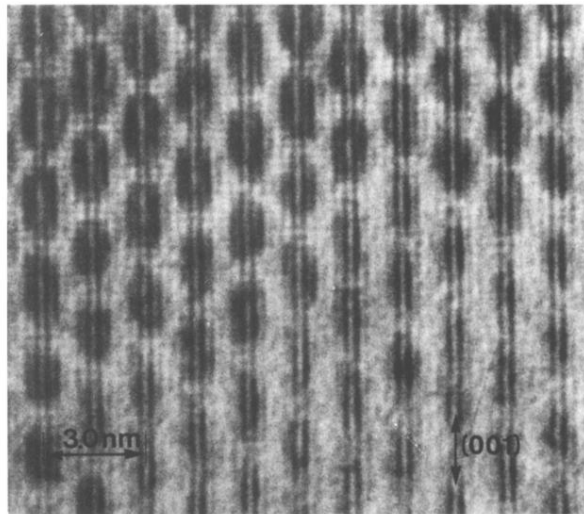


FIG. 3. High-resolution image along the [100] direction of the superlattice cell. The bismuth-containing layers are evident pairs of dark lines. Modulation of contrast along the lines suggests that there is a 25.8-Å modulation in the concentration of bismuth in these layers that is incommensurate with the perovskite substructure.